

Thermoelectric performance of classical topological insulator nanowires

Johannes Gooth^{1*}, Jan Göran Gluschke^{2,3}, Robert Zierold¹, Martin Leijnse², Heiner Linke², Kornelius Nielsch^{1#}

¹ *Institute of Applied Physics, Universität Hamburg, Jungiusstrasse 11, 20355 Hamburg, Germany*

² *Solid State Physics and Nanometer Structure Consortium (nmC@LU), Lund University, Box 118, S – 22100 Lund, Sweden*

³ *School of Physics, The University of New South Wales, Sydney NSW 2052, Australia*

ABSTRACT

We challenge the premise that the high thermoelectric performance of topological insulator chalcogenide-type materials in bulk remains unchanged on a nanometer scale (> 10 nm). In particular, we calculate the thermoelectric performance of topological insulator nanowires based on Bi_2Te_3 , Sb_2Te_3 and Bi_2Se_3 as a function of diameter and Fermi energy. For all investigated systems the competition between surface states and bulk channel causes a significant modification of the thermoelectric transport coefficients if the diameter is reduced into the sub-10 μm range, limiting the maximum thermoelectric performance of topological insulator nanowires and thus their application in efficient thermoelectric devices.

Electronic address: * jgooth@physnet.uni-hamburg.de
 # knielsch@physnet.uni-hamburg.de

Semiconductor nanowires have been predicted to significantly improve upon the corresponding bulk-material's efficiency of thermoelectric (TE) energy conversion,¹⁻³ quantified by the TE figure of merit $ZT = S^2\sigma T/(\kappa_{el}+\kappa_{ph})$, where T is the temperature, S denotes the Seebeck coefficient, σ the electrical conductivity, κ_{el} the electron thermal conductivity and κ_{ph} the phonon thermal conductivity. While the predicted power factor ($S^2\sigma$) enhancement due to 1D quantisation⁴⁻⁶ has yet to be observed and $S^2\sigma$ enhancement in nanowires due to quantum dot like states has only been achieved at low temperatures,⁷ it has been shown that utilizing the large surface to volume ratio s/v of nanowires enhancing phonon surface scattering can be used to decrease κ_{ph} .⁸⁻¹¹ A common approach intended to create high performance TE devices for room temperature operation is therefore to downscale materials with already high bulk ZT s to improve the TE performance. In particular chalcogenide nanowires based on Bi_2Te_3 , Sb_2Te_3 and Bi_2Se_3 have attracted special interest and inspired extensive research efforts because these compounds are associated with the highest room-temperature bulk TE efficiencies to date ($ZT \sim 1$).¹² Since ZT strongly depends on the Fermi energy of the investigated system, a specific strategy to achieve maximal performance in nano-scaled TE devices is therefore to synthesize nanowires with carrier concentrations optimized for maximum bulk ZT .¹³⁻¹⁵ However, while the expected reduction in κ_{ph} was observed in various thermoelectric transport experiments on such nanowires,¹⁶⁻¹⁹ S was reduced significantly,¹⁹⁻²³ resulting in a substantial decline of ZT (~ 0.1) compared to bulk values. In fact, for intrinsic Bi_2Te_3 nanowires (p-type in bulk) S was found to be negative (corresponding to n-type transport).^{21, 28} Here, we demonstrate that these experimental observations are an expected consequence of the recently discovered topological insulator (TI) nature of such

chalcogenide materials,²⁴⁻³⁸ because the TE performance of the bulk and the surface of the nanowires are optimized at different carrier concentrations (Fermi level positions E_F). Three dimensional TIs are a phase of matter with insulating bulk and gapless surface states that form a single Dirac cone, protected by time reversal symmetry which results in unique transport properties. While topological surface states play no role in TE transport in bulk materials, they may contribute substantially to the transport in nanostructures³⁹ due to their large surface to volume ratio. In fact, electrical transport experiments on Bi_2Te_3 ^{27, 28, 35} and $\text{Bi}_2\text{Se}_2\text{Te}$ ⁴⁰ nanowires revealed that the two-dimensional metallic TI surface channels contribute up to 30-70 % of the total electrical conduction at surface to volume ratios of $s/v = 2 - 5 \cdot 10^{-2} \text{ nm}^{-1}$. Previous theoretical studies on TE properties of TIs have shown that surface or edge states can in principle enhance the TE performance, for example on two-dimensional TIs with one dimensional edge states,^{41, 42} on three-dimensional TIs with line dislocations⁴³ as well as on Bi_2Te_3 and Bi_2Se_3 thin films.^{44, 45} These calculations focus on length scales below 10 nm, where hybridization of the topological states, resulting in a gap opening at the Dirac point, is expected to enhance the TE efficiency. Such sub-10 nm TE devices have to date not been realized, in part because of limitations in the template size or disturbances of the delicate equilibrium required in self-organized growth processes.⁴⁶ Due to its relevance for the material science community and for the ongoing development of Bi-Sb-Te-Se based TE nanostructures here we consider nanodevices with diameters above 10 nm at room-temperature. The thermoelectric performance in topological insulators strongly depends on the effective masses, carrier concentrations, bulk band gap and position of the Dirac

point. The Fermi energy E_F position is therefore an essential parameter in determining the TE performance of investigated material systems.

We have calculated the room temperature thermoelectric transport coefficients S , σ , κ_{el} and $ZT = S^2\sigma T/\kappa$ along the longitudinal axis of a single topological insulator nanowire in the diffusive limit as a function of E_F denoted relative to the valence band edge. Standard semi-classical Boltzmann equations under constant relaxation time approximation are used, considering two parallel, non-interacting channels as schematically shown in Fig. 1

(a): A three-dimensional semiconducting bulk channel with two parabolic bands (valence and conduction band) separated by a band gap ΔE_b and a two-dimensional gapless surface channel with a linear dispersion relation. The investigated nanowire diameters d lie well above the size range, in which confinement effects in the nanowire bulk¹ or hybridization of the surface states^{44, 47} might entail deviations from our calculation for Bi_2Te_3 , Sb_2Te_3 as well as for Bi_2Se_3 at 300 K. The detailed methods for calculating S , σ , κ and hence ZT as well as all model parameters—obtained from the literature—of the individual transport channels can be found in the supporting information.

For an anisotropic bulk crystal the thermoelectric efficiency ZT_b varies with transport direction, generally determined by the nanowire growth direction, which is expressed in a highly anisotropic effective mass tensor (see SI for details). Here, we choose to perform all calculations along the crystal orientation of highest mobility—parallel to the c-axis—and therefore along the direction of highest ZT_b to gain maximal bulk contribution in the total thermoelectric transport. Note, that the carrier mobility in nanostructures is generally suppressed compared to bulk values, due to enhanced surface scattering,⁴⁸ which could lead to an overestimation of the bulk contribution to the total electrical

transport in our calculations. Bulk Bi_2Te_3 , Sb_2Te_3 , and Bi_2Se_3 are narrow-band-gap semiconductors with band gaps of 105 meV, 90 meV, and 300 meV, respectively. The phonon contributions to the thermal conductivity κ_{ph} of the bulk channel were taken from literature and correspond to bulk materials. They do not account for a possible reduction of κ_{ph} in the nanowire e.g. due to enhanced surface scattering or impurities. We have chosen to provide both, the electronic part of the thermoelectric figure of merit $ZT_{\text{el}} = S^2\sigma T/\kappa_{\text{el}}$ as well as $ZT = S^2\sigma T/(\kappa_{\text{el}} + \kappa_{\text{ph}})$ in order to give an upper and lower limit for the actual TE performance of the nanowire bulk. We do, however, point that the substantial reduction of κ_{ph} due to phonon confinement is negligible for diameters above 10 nm.¹

The transport coefficients of the surface channel are expected to be independent of crystal orientation, due to the existence of TI states on all Bi_2Te_3 , Sb_2Te_3 and Bi_2Se_3 surfaces. To capture the transport of the Dirac particles at the surface of the nanowire, we chose a mean free path of 100 nm and a Fermi velocity of $4 \cdot 10^5 \text{ ms}^{-1}$.^{32, 33} The position of the Dirac point relative to the bulk valence band edge ΔE_{DP} has been experimentally determined by Angle Resolved Photoemission Spectroscopy as -265 meV for Bi_2Te_3 , -38 meV for Sb_2Te_3 and 145 meV for Bi_2Se_3 ,³³ exemplary representing materials with the Dirac point deeply buried in a bulk band (Bi_2Te_3), at the band edge (Sb_2Te_3) and the center of the band gap (Bi_2Se_3).

When calculating the total thermoelectric properties of a topological insulator, care must be taken in the qualitative comparison of the surface and bulk contributions because of the different dimensionality of the channels. The total electrical conductivity of a topological insulator is given by

$$\sigma = (G_{\text{b}} + G_{\text{s}}) \cdot \frac{L}{A} = \sigma_{\text{b}} + \sigma_{\text{s}} \frac{s}{v}. \quad (1)$$

G_b and G_s are the electrical conductances of the bulk and the surface channel, respectively; L denotes the length of the nanowire; A its cross-sectional area and s/v its surface-to-volume ratio. Of a (circular) nanowire with diameter d the surface-to-volume ratio accounts to $\frac{s}{v} = \frac{4}{d}$. The total Seebeck coefficient S of a topological insulator nanowire can straightforwardly be calculated within the two-channel model¹² as

$$S = \frac{S_b \sigma_b + S_s \sigma_s \frac{s}{v}}{\sigma_b + \sigma_s \frac{s}{v}} \quad (2)$$

S_b and S_s are the thermopowers of the bulk and the surface channel respectively. The total electronic part of the thermal conductivity¹² is calculated using

$$\kappa_{el} = \kappa_{el,b} + \kappa_{el,s} \frac{s}{v} + \frac{\sigma_b \cdot \sigma_s \frac{s}{v}}{\sigma_b + \sigma_s \frac{s}{v}} (S_s - S_b)^2 T. \quad (3)$$

κ_{el} consists of the individual electronic thermal conductivity of the bulk $\kappa_{el,b}$ and of the surface channel $\kappa_{el,s}$ as well as of an additional diffusion term that is enabled by the two different Seebeck coefficients of the surface states and of the bulk.¹² Note that the total Seebeck coefficient as well as the ratio of the electrical and thermal conductivity of a two channel system will never be larger than the maximum value of the individual channels (see SI for details). The TE efficiency of the bulk or surface states will therefore pose the limit of the TE efficiency of the total nanostructure.

Our calculations reveal that with decreasing diameter the thermoelectric transport in chalcogenide TI wires is increasingly dominated by the surface states. Since the TE performances of the bulk and of the surface states are optimized at different Fermi level positions, $S^2\sigma$ and ZT of TI wires with bulk-optimized carrier concentrations are significantly reduced at diameters in the sub-10 μm range, compared to bulk values. Additionally, the model explains the recently found negative Seebeck coefficient in

intrinsic Bi₂Te₃ nanowires (p-type in bulk).²¹ But even by readjusting the Fermi level for each diameter at the position of maximum TE performance, a significant degradation of the maximum thermoelectric performance in Bi₂Te₃ wires for $d < 10 \mu\text{m}$ is observed. We do, however, find an enhanced ZT compared to bulk, for Bi₂Se₃ nanowires in this diameter range with up to a three-fold enhancement at 10 nm diameter. Moreover, we show that regardless of precise shape or bulk material, the total thermoelectric efficiency of a topological insulator nanostructure with gapless states will eventually converge to the thermoelectric efficiency of the surface with decreasing system size.

The TE transport coefficients of each single channel behave as expected from literature. The thermoelectric figures of merit of the bulk channel $ZT_b(E_F)$ (Fig. 1(b)) as a function of Fermi energy reveal the characteristic double-peak structure of a two-band material, resulting from the line shape of the Seebeck coefficient $S_b(E_F)$ (Fig. 1(c)) weighted by the σ/κ -ratios (Fig. 1 (d),(e)). The asymmetry in $ZT_b(E_F)$ is caused by the different effective masses of the bulk valence and conductance bands. We obtain maximum bulk thermoelectric figures of merit of $ZT_b(E_{F,\text{opt,b}} = 155 \text{ meV}) = 0.84$ for n-type Bi₂Te₃, $ZT_b(E_{F,\text{opt,b}} = -54 \text{ meV}) = 0.16$ for p-type Sb₂Te₃, and $ZT_b(E_{F,\text{opt,b}} = 361 \text{ meV}) = 0.06$ for n-type Bi₂Se₃ at 300 K for optimal Fermi energies $E_{F,\text{opt,b}}$, corresponding to bulk carrier concentrations of $n_e = 1.11 \cdot 10^{20} \text{ cm}^{-3}$, $n_p = 1.28 \cdot 10^{19} \text{ cm}^{-3}$ and $n_e = 4.36 \cdot 10^{18} \text{ cm}^{-3}$, respectively. These values are in good agreement with literature.¹² Small deviations might occur due to slightly varying bulk parameters in literature. At the surface the symmetry of the Dirac cone generates two equally high maxima of $ZT_s(E_{F,\text{opt,s}}) = 0.26$ for electron and hole cone located at about 80 meV off the Dirac point, corresponding to a carrier concentration of $n_{e/p} = 2 \cdot 10^{12} \text{ cm}^{-2}$.

Combining surface and bulk channels, we find that the total thermoelectric properties of topological insulator Bi_2Te_3 , Sb_2Te_3 and Bi_2Se_3 wires are increasingly dominated by the surface states with decreasing diameter, as a simple consequence of enhancing surface to volume ratio. If the wire diameter is reduced below the 10 μm range, the competition between surface states and bulk channel causes a significant reshaping of the whole energy dependence of each individual transport coefficient as shown in Fig.2 and in SI Fig. 1. While the total electric (Fig. 2 (b),(g),(i)) and thermal conductivity (Fig. 2 (c),(h),(m)) continuously increases as the system-size is decreased, due to the mere fact that the metal-like surface states increasingly govern influence, the transformation of the thermopower (Fig. 2 (a),(f),(k)) depends on the Fermi energy, increasing or decreasing with declining nanowire diameter. A reduction of the total Seebeck coefficient has been observed in various experiments on Bi-Sb-Te-Se based nanostructures such as nanowires¹⁹⁻²³ and thin films.⁴⁹⁻⁵¹ For Sb_2Te_3 and Bi_2Te_3 the transformation of the energy landscape has an additional crucial impact: Below a nanowire diameter of about 200 nm, the thermopower becomes of negative sign for Fermi energies within the bulk valence band, because the Dirac point on the surface of Sb_2Te_3 and Bi_2Te_3 is located in the bulk valence band leading to a bipolar competition between electrons on the surface (negative Seebeck coefficient) and holes in the bulk (positive Seebeck coefficient). This finding possibly explains recent thermal²¹ and magnetotransport measurements²⁸ on Bi_2Te_3 nanowires, wherein a negative thermopower has been determined at Fermi energies deeply buried in the bulk valence band. The relative contribution of the surface states to the total electrical conductivity (Bi_2Te_3 : 15% for $d = 100$ nm at $E_F = -205$ meV) are in reasonably good agreement with experimental data.^{27, 28, 35} The herein presented

calculations are done for single-crystalline nanostructures with perfect surfaces and there are several possible reasons for why the relative contributions of the electronic thermal and electric conductivity could deviate in experiments: On the one hand, imperfections at the surface of the nanowire could lead to a lower surface mean free path than assumed in our model. On the other hand, additional scattering mechanisms in the bulk channel due to grain boundaries or surface roughness are known to decrease its electrical and thermal conductivity.⁸⁻¹¹ Although all listed effects would result in an overall reduction of the total electrical and thermal conductivity of the topological insulator nanowire, an increasing electrical and thermal conductivity with decreasing nanowire diameter seems to be a strong indication for topological surface states.

We now discuss the common experimental strategy to obtain the predicted high thermoelectric performances in nanowires by downscaling bulk material with carrier concentrations optimized for highest bulk ZT_b .¹³⁻¹⁵ In our calculation this experimental strategy is similar to a reduction of the nanowire diameter, fixing the Fermi energy that yields highest bulk efficiency $E_{F, \text{opt}, b}$ (see SI Fig. 2). Regardless of material, by downscaling the wire diameter into the nanometer range at $E_{F, \text{opt}, b}$ (i.e. carrier concentration) the thermopower as well as the TE efficiency is strongly suppressed compared to bulk values. The increasing electrical conductivity is compensated by the likewise increase of the thermal conductivity. In case of 100 nm diameter we obtain $ZT(E_{F, \text{opt}, b}) = 0.03$ for a n-type Bi_2Te_3 , $ZT(E_{F, \text{opt}, b}) = 0.06$ for a p-type Sb_2Te_3 and $ZT(E_{F, \text{opt}, b}) = 0.03$ for a n-type Bi_2Se_2 . The results reflect the overall experimental observations very well. A more detailed comparison of theory and experiment would require diameter dependent thermoelectric transport studies on nanowires at fixed Fermi

energies. Unfortunately such data is not available to date. An analogous system-size dependence is observed for the pure electronic ZT_{el} converging to similar values as obtained in the case of full phonon contribution below a system size of 100 nm.

The question thus arises whether topological insulator nanowires can reach bulk thermoelectric efficiency at all? The remarkable suppression of the thermoelectric efficiency in nanometer-scaled optimized bulk materials can be attributed to two main features (Fig. 2 (e),(j),(k); SI Fig. 1): first, to a narrowing of the ZT -peaks as the system size is reduced; and second, to a shift of the efficiency maximum in Fermi energy. Both effects warrant a very accurate repositioning of the Fermi energy at each nanowire diameter to maximize the thermoelectric performance at the specific system size. Tuning the Fermi energy (i.e. the carrier concentration) via field effect or doping has recently turned out to provide a powerful experimental tool to achieve maximum thermoelectric performance in semiconducting nanostructures.^{7, 52, 53} Following this route, we extract the maximum ZT and ZT_{el} at the optimized Fermi energy $E_{F,opt}$ for each nanowire diameter as shown in Fig. 3 (a) and (b). While a monotonic decrease of ZT_{el} can be seen for Sb_2Te_3 and Bi_2Se_2 with decreasing system size, a non-monotonic decrease is observed for Bi_2Te_3 . The ZT_{el} curves are shaped by the thermopower at $E_{F,opt}$ evolving from competing S_S and S_b . This is particularly evident for Bi_2Te_3 since the thermopower at the maximum surface and bulk efficiency oppose each other in sign. The bipolar crossover between p-type ZT_s maximum in the surface states and n-type ZT_b maximum in the bulk, results in a strong suppression of the total ZT_{el} compared to the maximum efficiency of each individual channel. In Sb_2Te_3 and Bi_2Se_2 the thermopower decreases monotonically from bulk values towards the Seebeck coefficients of the surface states, whereby both channels

reach maximum efficiency at thermopowers of the same sign. The relatively weak diameter dependence in Sb_2Te_3 nanowires is the consequence of a smaller overlap of the surface and the bulk efficiency peaks in energy, compared to Bi_2Se_3 . For all materials investigated, a non-monotonic relation between ZT and system size is obtained. A minimum splits the ZT curves into two distinct size ranges marking the crossover between surface state dominated transport in smaller systems ($d \ll 200$ nm) and bulk dominated transport ($d \gg 200$ nm) in larger systems. The dependence of ZT on the system size follows the same arguments as ZT_{el} , but the bulk channel is additionally weighted by κ_{ph} . κ_{ph} results in a suppression of ZT_{b} as well as in an overall suppression of the total nanowire efficiencies compared to ZT_{el} . This demonstrates that phonons still play a noticeable role in thermoelectric transport, even if topological surface states dominate the electronic transport properties of the nanowire. We find that nano-scaling Bi_2Te_3 leads to a ten to hundred-time degradation of the maximum thermoelectric performance compared to bulk. While Sb_2Te_3 seems to be relatively unaffected by size diameter variations, we receive, however, an up to three-fold enhanced ZT compared to bulk for Bi_2Se_3 . In all systems investigated, the maximum TE performances of the topological insulator nanowires converge towards the maximum TE performance of the surface states with decreasing diameter.

Our findings should generally apply for topological insulators of arbitrary geometry, such as thin films, membranes or nanotubes. This is expected, because the results obtained in our calculations are simply a matter of surface to volume ratio (Fig. 3 (c),(d)). Therefore, turning back to the initial question, in the presence of gapless surface states, the total thermoelectric efficiency of a topological insulator nanostructure will eventually

converge to the thermoelectric efficiency of the surface states with decreasing system size, regardless of precise shape or bulk material. However, the details of this process depend on the surface to volume ratio of the nanostructure, on ZT_b as well as on the relative position of the Dirac point to the bulk band structure. Topological insulator nanostructures with gapless surface states could therefore, on the one hand be a chance to enhance the thermoelectric performance of materials with $ZT_b > ZT_s$ and on the other hand pose a limit to the thermoelectric performance of materials with $ZT_b < ZT_s$. Nevertheless, the maximum TE surface efficiency of $ZT \sim 0.26$ is far below the highest room-temperature bulk TE efficiencies to date ($ZT \sim 1$) and requires accurate positioning of the Fermi level. Important for future applications will therefore be the suppression of topological surface states. Implementation of magnetic impurities on the surface of a topological insulator is known to break time reversal symmetry and thus to introduce a backscattering channel accompanied with a gap opening at the Dirac point.^{54, 55} In addition, recent calculations predict that the hybridization gap formed in ultrathin topological insulators with system sizes below 10 nm might provide a chance to improve their thermoelectric properties compared with bulk performances.⁴¹⁻⁴⁵ Topological insulator nanowires with diameters below 10 nm could hence be of high interest because hybridization of the surface states as well as quantum confinement in the bulk is proposed to significantly enhance the thermoelectric performance of each individual transport channel. However, in the diameter range experimentally achievable to date ($d > 10$ nm), the presents of gapless surface states limits the thermoelectric efficiency of topological insulator nanowires and thus their application in efficient thermoelectric devices. In this size range, alternative concepts utilizing confinement effects in nanometer-scaled non-

conventional good bulk thermoelectric materials, such as in InAs,⁷ ZnO and GaN⁵⁶ nanowires as well as in Ge-Si core-shell nanowires⁵² might pave the way to future TE application.

ACKNOWLEDGEMENTS

We thank Ulrich Merkt and Toru Matsuyama for useful discussions. This work was supported by the Deutsche Forschungsgemeinschaft (DFG) via Graduiertenkolleg 1286 “Functional Metal-Semiconductor Hybrid Systems“ and SPP 1666 “Topological insulators: Materials – Fundamental Properties –Devices”, by the Swedish Energy Agency (project 38331-19) as well as by the Swedish Foundation for Strategic Research.

REFERENCES

- [1] L. D. Hicks and M. S. Dresselhaus, *Phys. Rev. B* **47**, 16631 (1993).
- [2] N. Mingo, *Appl. Phys.Lett.* **84**, 2652 (2004).
- [3] J. E. Cornett and O. Rabin, *Appl. Phys.Lett.* **98**, 182104 (2011).
- [4] N. Neophytou and H. Kosina, *Phys. Rev. B* **83**, 245305 (2011).
- [5] N. Nakpathomkun, H. Q. Xu, and H. Linke, *Phys. Rev. B* **82**, 235428 (2010).
- [6] J. E. Cornett and O. Rabin, *Phys. Rev. B* **84**, 205410 (2011).
- [7] P. M. Wu et al., *Nano Lett.* **13**, 4080 (2013).
- [8] A. I. Hochbaum et al., *Nature* **451**, 163 (2008).
- [9] A. I. Boukai et al., *Nature* **451** 168 (2008).
- [10] F. Zhou et al., *Phys. Rev. B* **83**, 205416 (2011).
- [11] K. Nielsch, J. Bachmann, J. Kimling, and H. Boettner, *Adv. Energ. Mat.* **1**, 713 (2011).
- [12] G. S. Nolas, J. Sharp, and H. J. Goldsmid, *Thermoelectrics* (Springer-Verlag: Berlin Heidelberg, Germany, 2001).

- [13] G. Chen, M. S. Dresselhaus, G. Dresselhaus, J. P. Fleurial, and T. Caillat, *Intern. Mat. Rev.* **48**, 45 (2003).
- [14] M. S. Dresselhaus et al., *Adv. Mat.* **19**, 1043 (2007).
- [15] E. Pop, *Nano Res.* **3**, 147 (2010).
- [16] M. Munoz Rojo et al., *J. of Appl. Phys.* **113**, 054308 (2013).
- [17] G. D. Li, D. Liang, R. L. J. Qiu, and X. P. A. Gao, *Appl. Phys. Lett.* **102**, 043104 (2013).
- [18] D. Bessas et al., *Nanoscale* **5** 10629 (2013).
- [19] J. H. Zhou, C. G. Jin, J. H. Seol, X. G. Li and L. Shi, *Appl. Phys. Lett.* **87**, 133109 (2005).
- [20] A. Mavrokefalos et al., *J. of Appl. Phys.* **105**, 104318 (2009).
- [21] B. Hamdou et al., *Adv. Mat.* **25**, 239 (2013).
- [22] A. Purkayastha, F. Lupo, S. Kim, T. Borca-Tasciuc and G. Ramanath, *Adv. Mat.* **18**, 496 (2006).
- [23] S. Baessler et al., *Nanotechn.* **24**, 495402 (2013).
- [24] S. Matsuo et al., *Phys. Rev. B* **85**, 075440 (2012).
- [25] J. J. Cha et al., *Nano Lett.* **12**, 1107 (2012).
- [26] F. Xiu et al., *Nature Nanotechn.* **6**, 216 (2012).
- [27] M. Tian et al., *Sci. Rep.* **3**, 1212 (2013).
- [28] B. Hamdou, J. Gooth, A. Dorn, E. Pippel, and K. Nielsch, *Appl. Phys. Lett.* **103**, 193107 (2013).
- [29] B. Hamdou, J. Gooth, A. Dorn, E. Pippel, and K. Nielsch, *Appl. Phys. Lett.* **102**, 223110 (2013).

- [30] H. Peng, et al., *Nature Mat.* **9**, 225 (2010).
- [31] Y. L. Chen et al., *Science* **325**, 178 (2009).
- [32] D. Hsieh et al., *Phys. Rev. Lett.* **103**, 146401 (2009).
- [33] H. Zhang et al., *Nature Phys.* **5**, 438 (2009).
- [34] G. Q. Zhang, Q. X. Yu, W. Wang, and X. G. Li, *Adv. Mat.* **22**, 1959 (2010).
- [35] Y. Xia et al., *Nature Phys.* **5**, 398 (2009).
- [36] H. Steinberg, D. R. Gardner, Y. S. Lee and P. Jarillo-Herrero, *Nano Lett.* **10**, 5032 (2010).
- [37] S. S. Hong, J. J. Cha, D. Kong and Y. Cui, *Nature Comm.* **3**, 757 (2010).
- [38] D. Kong et al., *Nano Lett.* **10**, 329 (2010).
- [39] F. Rittweger, N. F. Hinsche, P. Zahn and I. Mertig, *Phys. Rev. B* **89**, 035439 (2014).
- [40] L. Bao et al., *Sci. Rep.* **2**, 726 (2012).
- [41] R. Takahashi and S. Murakami, *Phys. Rev. B* **81**, 161302 (2010).
- [42] R. Takahashi and S. Murakami, *Sem. Sci. and Techn.* **27**, 124005 (2012).
- [43] O. A. Tretiakov, A. Abanov, S. Murakami, and J. Sinova, *Appl. Phys. Lett.* **97**, 073108 (2010).
- [44] P. Ghaemi, R. S. K. Mong, and J. E. Moore, *Phys. Rev. Lett.* **105**, 166603 (2010).
- [45] Y.S. Horet al., *Phys.Rev. B* **79**, 195208 (2009).
- [46] L. Cademartiri and G. A. Ozin, *Adv. Mat.* **21**, 1013 (2009).
- [47] Y. Jiang et al., *Phys. Rev. Lett.* **108**, 016401 (2012).
- [48] E. H Sondheimer, *Adv. in Phys.* **1**, 1 (1952).
- [49] N. Peranio, O. Eibl, and J. Nurnus, *J. of Appl. Phys.* **100**, 114306 (2006).

- [50] S. Zastrow et al., *Semicon. Sci. and Techn.* **28**, 035010 (2013).
- [51] A. Boulouz et al., *J. of Appl. Phys.* **89**, 5009 (2001).
- [52] J. Moon, J.-H. Kim, Z. C. Y. Chen, J. Xiang, and R. Chen, *Nano Lett.* **13**, 1196 (2013).
- [53] S. Roddaro et al., *Nano Lett.* **13**, 3638 (2013).
- [54] H. T. He et al., *Phys. Rev. Lett.* **106**, 166805 (2011).
- [55] Q. Liu, C.-X. Liu, C. Xu, X.-L. Qi and S.-C.Zhang, *Phys. Rev. Lett.* **102**, 156603 (2009).
- [56] C.-H. Lee, G.-C. Yi, Y. M. Zuev and P. Kim, *Appl. Phys. Lett.* **94**, 022106 (2009).

FIGURES

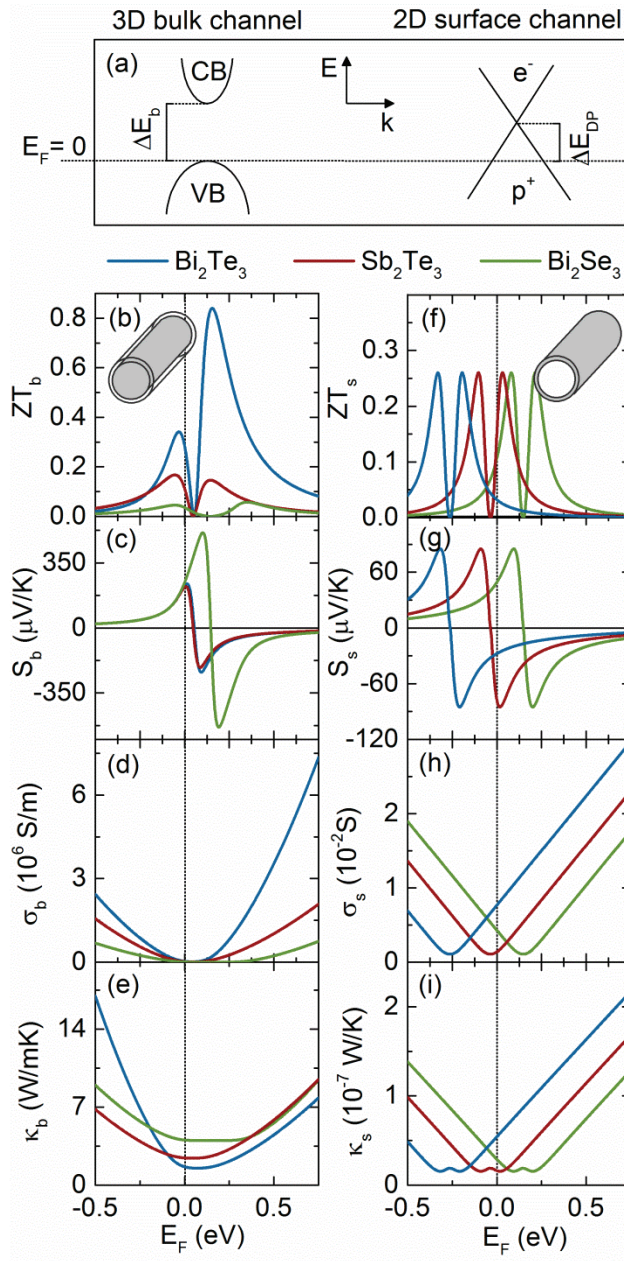


FIG 1. Thermoelectric transport coefficients of the bulk (right) and of the surface (left) channel of topological insulator Bi_2Te_3 (blue), Sb_2Te_3 (red) and Bi_2Se_3 (green) nanowires. Bulk and surface channel correspond to the subscripts b and s respectively. (a) The three-dimensional bulk channel is a two-band semiconductor with parabolic

dispersion relation, where the two bands (valence (VB) and conduction band (CB)) are separated by a bandgap ΔE_b . The two-dimensional surface channel is characterized by a gapless Dirac cone (linear dispersion relation) with electron states (e^-) on one side of the Dirac point and hole states (p^+) on the other. ΔE_b is the distance between the Dirac point and the bulk valence band edge. (b), (f) The thermoelectric figure of merit ZT , (c), (g) the thermopower S as well as the (d), (h) electrical σ and (e), (i) thermal conductivity κ of both channels are calculated as a function of the Fermi energy E_F , measured relative to the bulk valence band edge.

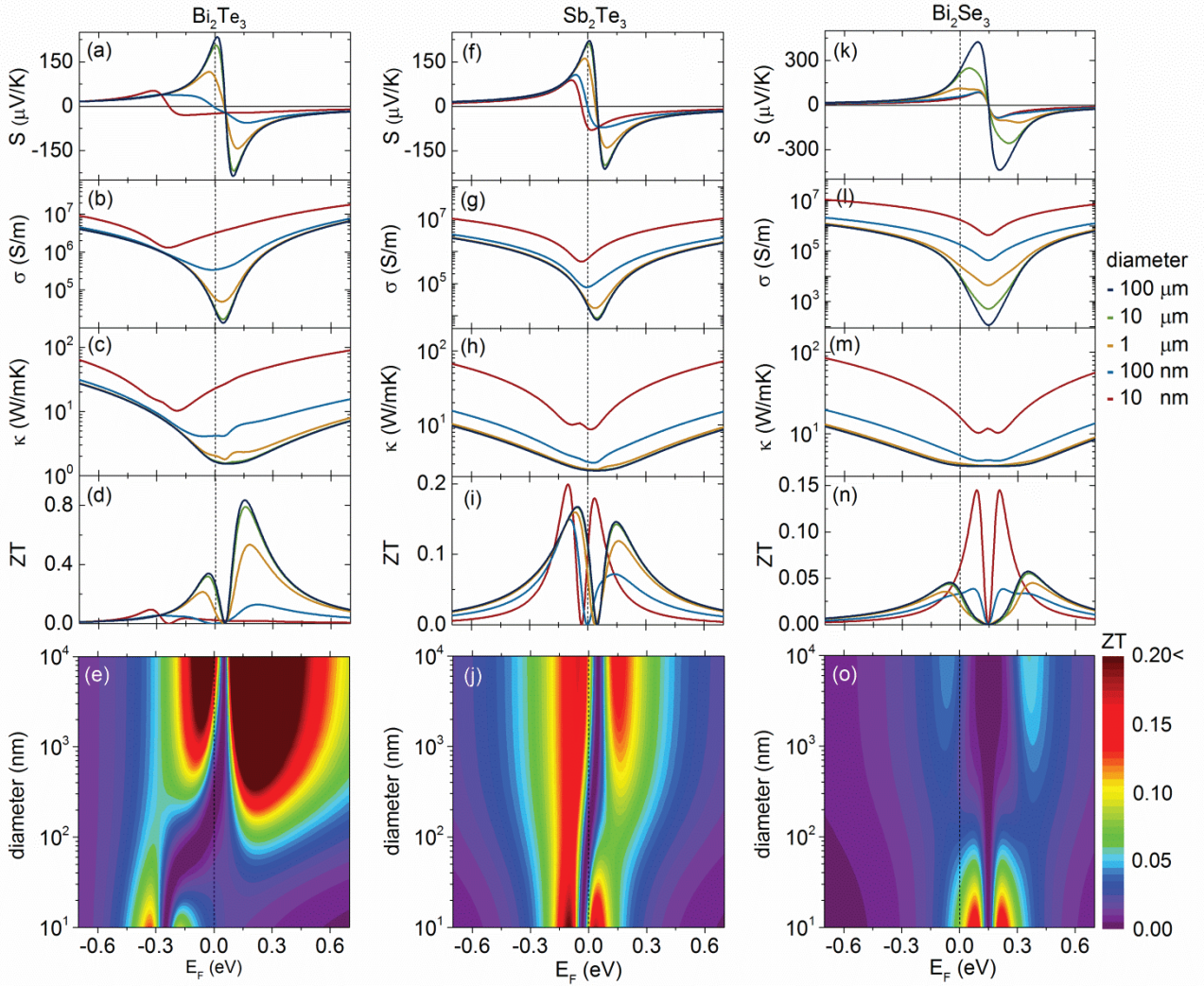


FIG 2. Diameter-dependent thermoelectric transport coefficients of topological insulator Bi_2Te_3 , Sb_2Te_3 and Bi_2Se_3 nanowires (from left to right column). (a), (f), (k) Thermopower S ; (b),(g),(l) electrical conductivity σ ; (c), (h), (m) thermal conductivity κ ; and (d), (i), (n) thermoelectric figure of merit ZT at 300 K are plotted as a function of Fermi energy, relative to the bulk valence band edge ($E_F = 0$ eV). (e), (j), (o) ZT is plotted as function of diameter and Fermi energy in a two-dimensional color plot. When the wire diameter is reduced the competition between surface states and bulk channel causes a significant reshaping of the whole energy dependence of each individual transport

coefficient. With decreasing wire diameter the thermoelectric transport is increasingly dominated by the surface states as a simple consequence of increasing surface to volume ratio. A remarkable suppression of the thermoelectric efficiency is observed if E_F is at a position optimized for bulk material: first, because of narrowing of the ZT -peaks as the system nanowire diameter is reduced; and second, because of a shift of the efficiency maximum in Fermi energy.

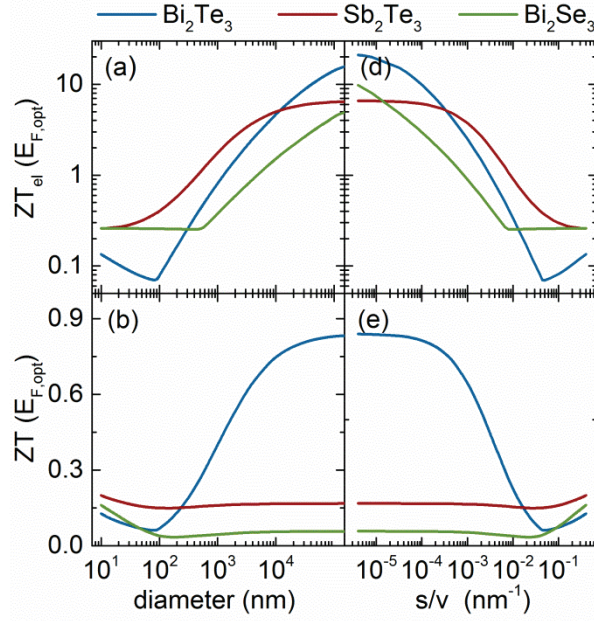


FIG 3. Maximum electronic thermoelectric figure of merit $ZT_{el}(E_{F,opt}) = S^2\sigma/\kappa_{el}$ and maximum thermoelectric figure of merit $ZT(E_{F,opt}) = S^2\sigma/(\kappa_{el} + \kappa_{ph})$ at optimized Fermi level position $E_{F,opt}$ of a topological insulator Bi_2Te_3 (blue), Sb_2Te_3 (red) and Bi_2Se_3 (green) nanowire as a function of diameter (left) and surface to volume ratio (right). Regardless of precise shape or bulk material, the total thermoelectric efficiency of a topological insulator nanostructure with gapless surface states will eventually converge to the thermoelectric efficiency of the surface with decreasing system size.

Supporting information for the manuscript

Thermoelectric performance of classical topological insulator nanowires

By Johannes Gooth, Jan Göran Gluschke, Robert Zierold, Martin Leijnse, Heiner Linke and Kornelius Nielsch

I. Boltzmann transport equations of the individual channels

All calculations are performed using Boltzmann transport equations under the assumption of a constant relaxation time τ . The electrical conductivity σ , the thermopower S and the electronic contribution of the thermal conductivity κ_{el} for electrons (-) or holes (+) are expressed by

$$\sigma = e^2 \cdot X_0 \quad (1)$$

$$S = \pm \frac{1}{eT} \left(\frac{X_1}{X_0} - E_F \right) \quad (2)$$

$$\kappa_{\text{el}} = \frac{1}{T} \left(X_2 - \frac{X_1^2}{X_0} \right) \quad (3)$$

with $X_s = \int_{-\infty}^{\infty} \left(-\frac{\partial f}{\partial E} \right) \theta(E) E^s dE$ and $\theta(E) = g(E) v_x \tau$, where $g(E)$ is the density of states and v_x denotes the velocity of the charge carriers in x-direction.¹

Thermoelectric transport coefficients of the bulk channel.

The thermopower S_b , the electrical conductivity σ_b and the electronic thermal conductivity $\kappa_{b,\text{el}}$ of the bulk channel are calculated for an anisotropic three-dimensional semiconducting material, where the two bands (valence and the conduction band) are separated by a bandgap ΔE_b . Since the bands are assumed to be parabolic, the electronic dispersion relation of each bulk band is:

$$\epsilon(k_x, k_y, k_z) = \frac{\hbar^2 k_x^2}{2m_x} + \frac{\hbar^2 k_y^2}{2m_y} + \frac{\hbar^2 k_z^2}{2m_z} \quad (4)$$

Using the three-dimensional density of states $g(E) = \frac{(2m^*)^{3/2}}{2\pi^2\hbar^3} E^{1/2}$, with $m^* = (m_x m_y m_z)^{1/3}$ and expressing v_x and τ by the effective mass components m_x, m_y, m_z in x-,y-,z-direction and by the mobility μ_x in x-direction one obtains for the thermoelectric transport coefficients of each band along the x-direction (details of the transformation can be found elsewhere)^{1, 2}:

$$\sigma_{b,e/p} = \frac{e\mu_x}{2\pi^2} \left(\frac{2k_B T}{\hbar^2} \right)^{2/3} (m_x m_y m_z)^{1/2} F_{1/2}, \quad (5)$$

$$S_{b,e/p} = \pm \frac{k_B}{e} \left(\frac{5}{3} \frac{F_{3/2}}{F_{1/2}} - \gamma \right), \quad (6)$$

$$k_{el,b,e/p} = \frac{\mu_x m_x k_B \hbar^2}{6e\pi^2} \left(\frac{2k_B T}{\hbar^2} \right)^{5/3} \left(\frac{m_y m_z}{m_x} \right)^{1/2} \left(\frac{7}{2} F_{5/2} - \frac{25}{62} \frac{F_{3/2}^2}{F_{1/2}} \right), \quad (7)$$

where the subscripts e and p correspond to the conduction and the valence band respectively.

The Fermi-Dirac integral F_i of order i is given by

$$F_i(\gamma) = \int_0^\infty \frac{x^i dx}{e^{(x-\gamma)+1}} \quad (8)$$

$\gamma = E/k_B T$ is the reduced energy, with $E = -E_F$ for the valence band and $E = E_F - \Delta E_b$, the conduction band, where E_F is the Fermi energy relative to the edge of the valence band and T the absolute temperature. The total electrical conductivity of the bulk channel σ_b is the sum of the two band contributions $\sigma_b = \sigma_{b,e} + \sigma_{b,p}$. The total thermopower S_b and the total electronic thermal conductivity of a two band system is given by $S_b = (S_{b,e} \sigma_{b,e} + S_{b,p} \sigma_{b,p}) / (\sigma_{b,e} + \sigma_{b,p})$ and $\kappa_{el,b} = \kappa_{el,b,e} + \kappa_{el,b,p} + (\sigma_{b,e} \sigma_{b,p}) / (\sigma_{b,e} + \sigma_{b,p}) (S_{b,e} - S_{b,p})^2 T$ respectively. The phonon thermal conductivity $\kappa_{ph,b}$, is independent of the position of the Fermi energy. Finally, the bulk thermoelectric figure of merit for transport in x-direction can be calculated as

$$ZT_b = \frac{S_b^2 \sigma_b}{k_{el,b} + k_{ph,b}} T \quad (10)$$

For an anisotropic crystal the bulk ZT_b varies with transport direction. We choose to perform all calculations along the crystal orientation of highest mobility μ_x – parallel to the c-axis – and therefore along the direction of highest ZT_b to gain maximal bulk contribution in the total thermoelectric transport of the nanowire. μ_x is assumed to be equal for electrons and holes

(Bi_2Te_3 :¹ $\mu_x = 1200 \text{ cm}^2\text{V}^{-1}\text{s}^{-1}$, Sb_2Te_3 :¹ $\mu_x = 3500 \text{ cm}^2\text{V}^{-1}\text{s}^{-1}$ and Bi_2Se_3 :³ $\mu_x = 600 \text{ cm}^2\text{V}^{-1}\text{s}^{-1}$). The bandgaps of bulk Bi_2Te_3 , Sb_2Te_3 and Bi_2Se_3 are 105 meV, 90 meV and 300 meV respectively, and phonon thermal conductivities $\kappa_{\text{b,ph}}$ of $1.5 \text{ Wm}^{-1}\text{K}^{-1}$ for Bi_2Te_3 ,⁴ $2.4 \text{ Wm}^{-1}\text{K}^{-1}$ for Sb_2Te_3 ,⁴ and $4.0 \text{ Wm}^{-1}\text{K}^{-1}$ for Bi_2Se_3 ⁵ are used in our calculations. The effective mass tensors of Bi_2Te_3 , Sb_2Te_3 and Bi_2Se_3 are highly anisotropic and differ for valence (VB) and conduction band (CB), taken from table 1:

	Bi_2Te_3		Sb_2Te_3		Bi_2Se_3	
	VB	CB	VB	CB	VB	CB
$\mathbf{m}_x(\mathbf{m}_0)$	-0.024	0.178	-0.054	0.045	-0.125	0.109
$\mathbf{m}_y(\mathbf{m}_0)$	-0.134	0.178	-0.054	0.045	-0.125	0.122
$\mathbf{m}_z(\mathbf{m}_0)$	-1.921	0.835	-0.102	0.114	-0.125	0.24

Table 1: Components of the effective mass tensors for valence (VB) and conduction band (CB) of Bi_2Te_3 ,⁶ Sb_2Te_3 ,⁶ and Bi_2Se_3 .⁵ The effective mass tensor of the valence band in Bi_2Se_3 is isotropic.

Thermoelectric transport coefficients of the surface states.

The thermoelectric transport coefficients S_s , σ_s and κ_s of the surface channel are calculated for an isotropic two-dimensional gapless Dirac system relative to the valence band edge of the bulk channel, with a circular Fermi surface and linear dispersion relation $\epsilon(k) = \hbar k v_F$, where $v_F = 4 \cdot 10^5 \text{ ms}^{-1}$ is the Fermi velocity of the Dirac particles.^{7, 8} The contribution of the surface channel is expected to be independent of crystal orientation, due to the existence of surface states on all Bi_2Te_3 , Sb_2Te_3 and Bi_2Se_3 surfaces. The position of the Dirac point relative to the bulk valence band edge ΔE_{DP} has been taken from literature as -265 meV for Bi_2Te_3 , -38 meV for Sb_2Te_3 and 145 meV for Bi_2Se_3 .⁸ The thermopower S_s , the electrical conductivity σ_s and the electronic thermal conductivity $\kappa_{s,\text{el}}$ of one side of the Dirac cone are

calculated using equation (1), (2) and (3) with the two dimensional density of states $g(E) = \frac{E}{\pi(\hbar v_F)^2}$, the Fermi velocity $v_x = v_F$ and the relaxation time $\tau = \lambda/v_F$. Here we representatively choose the mean free path λ in the surface states to be $\lambda = 200$ nm, experimentally determined by several Aharonov-Bohm measurements.⁹⁻¹¹ The transport coefficients of the electrons in the Dirac cone are calculated, using $E = E_F + \Delta E_{DP}$ and of the holes, using $E = -E_F + \Delta E_{DP}$. The total electrical conductivity of the surface channel σ_s is the sum of the electron and hole contribution $\sigma_s = \sigma_{s,e} + \sigma_{s,p}$. The total thermopower S_s and the total electronic thermal conductivity of a two band system is given by $S_s = (S_{s,e} \sigma_{s,e} + S_{s,p} \sigma_{s,p}) / (\sigma_{s,e} + \sigma_{s,p})$ and $\kappa_{el,s} = \kappa_{el,s,e} + \kappa_{el,s,p} + (\sigma_{s,e} \sigma_{s,p}) / (\sigma_{s,e} + \sigma_{s,p}) (S_{s,e} - S_{s,p})^2 T$ respectively. The phonon thermal conductivity of the surface is assumed to be zero. Finally $ZT_s = S_s^2 \sigma_s / \kappa_{el,s}$ of the surface channel has been calculated. In reality the surface channel is not infinitely thin: the penetration depth of the surface states into the bulk is about 1 nm, which might cause a maximum-error of 20% in the diameter for the thinnest nanowires considered.

II. Maximum thermoelectric performance of a two-channel system

Here we address the maximum thermoelectric efficiency $max[ZT] = max[S^2 G / (K_{el} + K_{ph})]$ of a system with two parallel contributing transport channels (channel I and II) with individual thermoelectric efficiencies $ZT_I = S_I^2 G_I / (K_{el,I} + K_{ph,I})$ and $ZT_{II} = S_{II}^2 G_{II} / (K_{el,II} + K_{ph,II})$ where $S_{I/II}$ is the thermopower, $G_{I/II}$ the electrical conductance, $K_{el,I/II}$ the electronic and $K_{ph,I/II}$ the phonon thermal conductivity of transport channel I/II. We divide the problem of maximum ZT into two separated problems: Maximum S^2 and maximum $G / (K_{el} + K_{ph})$. The thermopower of a system with two parallel contributing transport channels is given by

$$S = \frac{S_I G_I + S_{II} G_{II}}{G_I + G_{II}}$$

Now we express each individual thermoelectric transport coefficient by the ratio between the transport coefficients of channel I and II. There are two possible scenarios: First, that the channel of highest thermopower has the higher electrical conductance. In this case $S_{II} = x \cdot S_I$, with $-1 \leq x \leq 1$, because $|S_I| \leq |S_{II}|$ and $G_{II} = y \cdot G_I$, with $0 \leq y \leq 1$, because $G_I \leq G_{II}$ leads to $S = \frac{1 \pm yx}{1+y} \cdot S_I$. Second, that the channel of highest thermopower has the lower electrical conductance. In this case $S_{II} = x \cdot S_I$, with $-1 \leq x \leq 1$, because $|S_I| \leq |S_{II}|$ and $G_{II} \cdot y = G_I$, with $0 \leq y \leq 1$, because $G_I \geq G_{II}$, leads to $S = \frac{x+y}{1+y} \cdot S_I$. Note that the channel of higher transport coefficient is arbitrary and could be reversed as well. Since in both scenarios $-1 \leq x \leq 1$ and $0 \leq y \leq 1$, consequently $1 + yx \leq 1 + y$ and $x + y \leq 1 + y$, leading to $\left| \frac{1+yx}{1+y} \right| \leq 1$ as well as $\left| \frac{x+y}{1+y} \right| \leq 1$. The total thermopower of the two-channel system will therefore never be larger than the highest value of the single channels:

$$|S| \leq \max[|S_I|, |S_{II}|]$$

This is particularly evident for transport channels with thermopowers that oppose each other in sign. The maximum $|S|$ is reached if the thermovoltages of both channels are similar ($x \rightarrow 1$).

The ratio of electrical and thermal conductance of a system with two parallel contributing transport channels is given by

$$\frac{G}{K_{el} + K_{ph}} = \frac{G_I + G_{II}}{K_{el,I} + K_{el,I} + \frac{G_I + G_{II}}{G_I \cdot G_{II}} (S_{II} - S_I)^2 \cdot T + K_{ph,I} + K_{ph,II}}$$

Since $\frac{G_I + G_{II}}{G_I \cdot G_{II}} (S_{II} - S_I)^2 T \geq 0$:

$$\frac{G}{K_{el} + K_{ph}} \leq \frac{G_I + G_{II}}{K_{el,I} + K_{el,I} + K_{ph,I} + K_{ph,II}} = \frac{G_I + G_{II}}{K_I + K_{II}} = \frac{\frac{G_I}{K_I}}{1 + \frac{K_{II}}{K_I}} + \frac{\frac{G_{II}}{K_{II}}}{1 + \frac{K_I}{K_{II}}}$$

Note, that $\frac{G_I+G_{II}}{G_I \cdot G_{II}} (S_{II} - S_I)^2 T = 0$ is the case for maximum thermopower.

Since $\frac{\frac{G_I+G_{II}}{K_I+K_{II}}}{\frac{G_I}{K_I}} = \frac{K_I+K_{II} \cdot \left(\frac{G_I}{K_I}\right) / \left(\frac{G_{II}}{K_{II}}\right)}{K_I+K_{II}} \begin{cases} > 1, \text{ for } \frac{G_I}{K_I} > \frac{G_{II}}{K_{II}} \\ < 1, \text{ for } \frac{G_I}{K_I} < \frac{G_{II}}{K_{II}} \end{cases}$, which holds reversed for channel II as

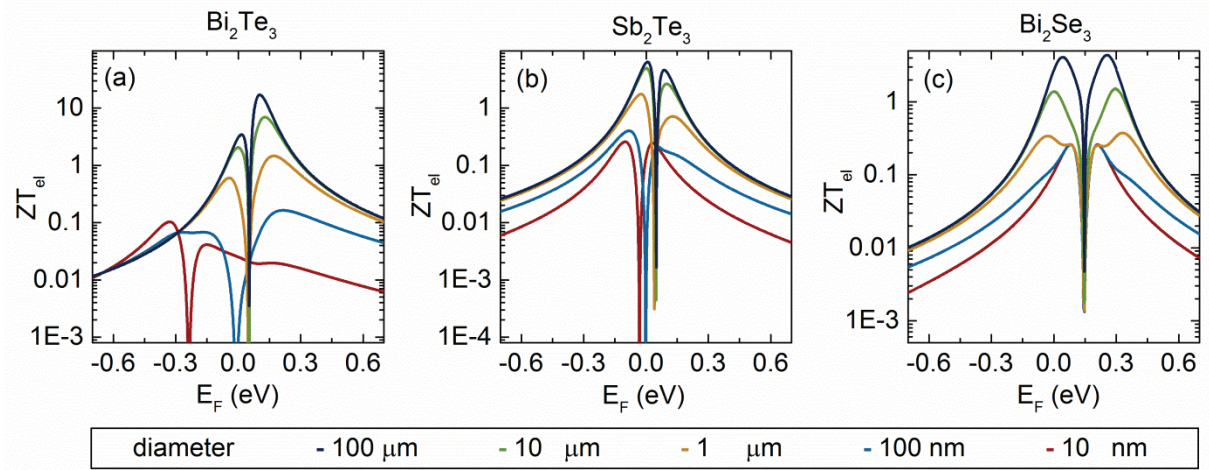
well, $\frac{G_I+G_{II}}{K_I+K_{II}}$ will never be higher than the maximum ratio of electrical and thermal conductance of a single channel $\max\left[\frac{G_I}{K_I}, \frac{G_{II}}{K_{II}}\right]$. Therefore the ratio of electrical and thermal conductance of a system with two parallel contributing transport channels will never be higher than the higher ratio of electrical and thermal conductance of the single channels:

$$\frac{G}{K_{el} + K_{ph}} \leq \max\left[\frac{G_I}{K_{el,I}+K_{ph,I}}, \frac{G_{II}}{K_{el,II}+K_{ph,II}}\right]$$

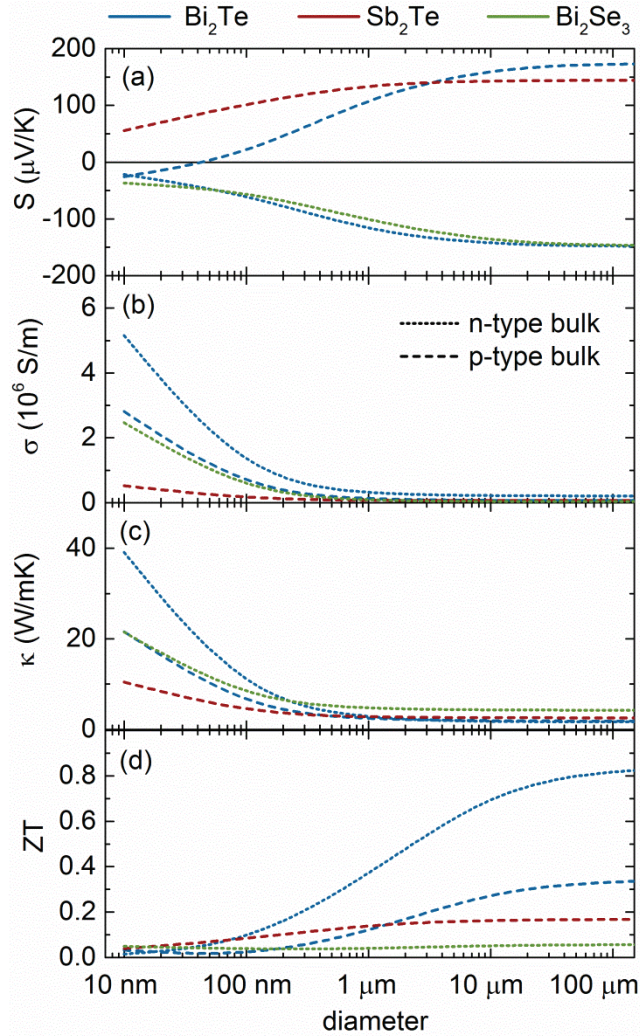
Consequently, the maximum thermoelectric efficiency $\max[ZT] = \max[S^2 G / (K_{el} + K_{ph})]$ of a system with two parallel contributing transport channels (channel I and II) will never exceed the maximum thermoelectric efficiency of the single channels $\max[ZT_I, ZT_{II}]$:

$$\max[ZT] \leq \max[ZT_I, ZT_{II}]$$

Best thermoelectric performance in a two-channel system is achieved if $S_I = S_{II}$ (leading to the maximum total thermopower) and $\frac{G_I}{K_I} = \frac{G_{II}}{K_{II}}$ (leading to the maximum ratio of electrical and thermal conductance).



SI FIG 1. Electronic thermoelectric figures of merit $ZT = S^2\sigma/\kappa_{\text{el}}$ of topological insulator (a) Bi_2Te_3 , (b) Sb_2Te_3 and (c) Bi_2Se_3 nanowires as a function of Fermi energy E_F at various diameters (color-coded).



SI FIG 2. Diameter dependent thermoelectric transport coefficients of topological insulator Bi_2Te_3 , Sb_2Te_3 and Bi_2Se_3 nanowires (dashed lines: Bi_2Te_3 (blue) and Sb_2Te_3 (red) with n-type bulk; dotted lines: Bi_2Te_3 (blue) and Bi_2Se_3 (green) with p-type bulk). The Fermi level is fixed at the position of maximum bulk ZT . Each transport coefficient shows a characteristic dependence on the nanowire diameter under the existence of topological surface states due to the shifting dominance of the bulk channel at large nanowire diameters towards the surface channel at small diameters as a simple consequence of increasing surface to volume ratio. (a) The thermopower S continuously increases for the nanowires with n-type bulk and decreases for the nanowires with p-type bulk. In Bi_2Te_3 the position of Dirac point in the bulk valence

band leads to a sign change in S . The thermoelectric figure of ZT as well as (d) the thermopower $|S|$ (without zero crossing) consciously decreases with decreasing nanowire diameter. (c) The electrical conductivity σ and the thermal conductivity (d) κ both increase with decreasing diameter. Independent of whether phonons contribute to the thermal transport in the nanowires or not.

REFERENCES

- [1] G. S. Nolas, J. Sharp and H. J. Goldsmid, *Thermoelectrics* (Springer-Verlag: Berlin Heidelberg, Germany, 2001).
- [2] L. D. Hicks and M. S. Dresselhaus, *Phys. Rev. B* **74**, 16631 (1993).
- [3] J. A. Woollam, I. L. Spain and H. Beale, *Phys.Lett.A* **41**, 319 (1972).
- [4] D. Bessas et al., *Phys. Rev. B* **86**, 224301 (2012).
- [5] O. Madelung, *Non-Tetrahedrally Bonded Elements and Binary Compounds I* (Springer-Verlag: Berlin Heidelberg, Germany, 1998).
- [6] B. Y. Yavorsky, N. F. Hinsche, I. Mertig and P. Zahn, *Phys. Rev. B* **84**, 165208 (2011).
- [7] D. Hsieh et al., *Phys. Rev. Lett.* **103**, 146401 (2009).
- [8] H. Zhang et al., *Nature Phys.* **5**, 438 (2009).
- [9] M. Tian et al., *Sci. Rep.* **3**, 1212 (2013).
- [10] B. Hamdou, J. Gooth, A. Dorn, E. Pippel and K. Nielsch, *Appl. Phys. Lett.* **103**, 193107 (2013).
- [11] Y. Xia et al., *Nature Phys.* **5**, 398 (2009).